Sleep Medicine 48 (2018) 70–78

Contents lists available at ScienceDirect

Sleep Medicine

journal homepage: www.elsevier.com/locate/sleep

Original Article

Detecting inspiratory flow limitation with temporal features of nasal airflow

Ying Xuan Zhi [a, b], Daniel Vena [a, b], Milos R. Popovic [a, b], T. Douglas Bradley [a, c, d], Azadeh Yadollahi [a, b, *]

[a] University Health Network, Toronto Rehabilitation Institute, 550 University Ave., Toronto, Canada
[b] Institute of Biomaterials and Biomedical Engineering, University of Toronto, Toronto, Canada
[c] Centre for Sleep Medicine and Circadian Biology, University of Toronto, Toronto, Canada
[d] Department of Medicine, University Health Network, Toronto General Hospital, Toronto, Canada

ARTICLE INFO

Article history:
Received 30 September 2017
Received in revised form
1 March 2018
Accepted 17 April 2018
Available online 2 May 2018

Keywords:
Inspiratory flow limitation
Nasal airflow
Temporal features
Machine learning
Classification

ABSTRACT

Background: Inspiratory flow limitation is a breathing pattern during sleep caused by upper airway (UA) narrowing that occurs during snoring and various degrees of obstructive sleep apnea (OSA). Clinical examination of flow limitation relies on identifying patterns of airflow contour, however this process is subjective and lacks physiological evidence of UA narrowing. Our objective is to derive the temporal features of nasal airflow contour that characterize flow limitation. The features that correlate with UA narrowing can be used to develop machine learning classifiers to detect flow limitation with physiological support.
Methods: Sixteen healthy adult men underwent full daytime polysomnography where the nasal airflow was recorded. Before and after sleep, we measured UA anatomical parameters including neck circumference (NC) and upper-airway cross-sectional area (UA-XSA). We extracted various temporal features of airflow and investigated their relationships with the UA anatomical parameters.
Results: We found that three features were correlated with the anatomical parameters associated with UA narrowing: deviation index vs. baseline UA-XSA ($r = -0.67$, $p = 0.01$), peak amplitude variability vs. baseline UA-XSA ($r = -0.69$, $p < 0.01$), peak amplitude variability vs. ΔNC ($r = 0.74$, $p < 0.01$) and peak number vs. baseline UA-XSA ($r = -0.54$, $p = 0.04$).
Conclusions: Temporal features of airflow were associated with UA narrowing. Future studies could utilize the features to develop classifiers to detect flow limitation and assess the severity of breathing disorders during sleep in high-risk populations such as pregnant women and children.

1. Introduction

Inspiratory flow limitation (referred to as flow limitation in the text) during sleep is a common phenomenon that arises from upper airway (UA) narrowing. It occurs in various breathing disorders during sleep, ranging from snoring to varying degrees of obstructive sleep apnea (OSA). Normally with a patent UA, inspiratory airflow through the UA is proportional to the negative intrathoracic pressure. In contrast, flow limitation occurs when more negative intrathoracic pressure does not cause a corresponding increase in airflow [1]. Flow limitation is associated with reduced airflow, carbon dioxide (CO_2) retention, hypoxia, and elevated respiratory effort that can trigger arousals which, in turn, cause resolution of flow limitation by activating the upper airway dilator muscles [2,3]. The detrimental health effects related to flow limitation include disturbed sleep structure and daytime sleepiness [3]. Moreover, a recent study on the pathophysiology of flow limitation during sleep indicated that flow limitation is related to palatal anatomical abnormalities such as a thick palate and a voluminous lateral pharyngeal wall [4]. Although the presence of flow limitation in breathing disorders during sleep is widely acknowledged, the American Academy of Sleep Medicine currently recognizes flow limitation only as a manifestation of OSA; and no standard criteria have been established to evaluate its presence and severity [5,6].

* Corresponding author. University Health Network, Toronto Rehabilitation Institute, Institute of Biomaterials & Biomedical Engineering, University of Toronto, Room 12-106, 550 University Ave., Toronto, ON, M5G 2A2, Canada. Fax: +1 416 597 8959.
E-mail addresses: derek.zhi@mail.utoronto.ca (Y.X. Zhi), dvena@bwh.harvard.edu (D. Vena), milos.popovic@uhn.ca (M.R. Popovic), douglas.bradley@uhn.ca (T.D. Bradley), azadeh.yadollahi@uhn.ca (A. Yadollahi).

https://doi.org/10.1016/j.sleep.2018.04.006
1389-9457/

Conventionally, detection of flow limitation requires recordings of airflow and respiratory drive measured by pneumotachography and esophageal manometry, respectively [7]. However, these measurements are cumbersome and invasive. Alternatively, flow limitation can be inferred from airflow tracings that exhibit flattening or scooping patterns [8,9]. The airflow can be conveniently recorded by a noninvasive nasal cannula/pressure transducer system. In addition, the American Thoracic Society proposed methods to standardize the scoring of flow limitation from nasal airflow recordings, leading to a future focus of developing automated scoring algorithms [5]. Norman et al., designed a classifier using artificial neural network that was trained by manual annotation exacted from experts who visually examined the airflow contours [10]. Their proposed method achieved a classification agreement of 82.4% against the manual annotation, but the inter-annotator agreement for flow limited breaths was 80.3%. It was possible that the annotator-dependent bias reduced the classification accuracy. To preclude this bias, another study automatically clustered airflow contours into seven classes and interpreted the UA flow anatomic abnormality for each class [11]. While this study is exempt from the subjectivity of manual annotation, the author only posited the link between different clusters and the UA narrowing without actually assessing UA narrowing. Therefore, it is important to design studies to validate noninvasive detection of flow limitation based on assessment of the UA narrowing.

Direct measurements of UA narrowing such as MRI or UA endoscopy are expensive, cumbersome, and may alter sleep structures. To address this limitation, the present study aims to identify temporal features of airflow that characterize flow limitation and its association with UA narrowing. Previous studies from our group have shown that rostral fluid shift during sleep contributes to the UA narrowing. When moving from upright to recumbent position at bedtime, fluid that has accumulated in the legs during the day due to gravity moves out of the legs, and a part of this fluid accumulates in the neck by gravity, which increases neck circumference (NC) [12–14] and tissue pressure around the UA, which narrows the UA [15]. We assessed the severity of UA narrowing by measurements of NC and UA cross-sectional area (UA-XSA) before and after sleep. To characterize flow limitation, we calculated several temporal features of the airflow contour and investigated the relationship between these features and the UA parameters. To further validate these features, we used a clustering technique to separate breaths into flow limited and normal breaths and identified differences in the features between the clusters.

2. Method

2.1. Data collection

This is a retrospective study and data were extracted from a previous protocol, which was a double crossover study that investigated the effects of intravenous fluid infusion of approximately 2 L during sleep on sleep apnea severity [16]. For this study, we used data from the control arm of the previous protocol in which an intravenous line was inserted but saline was infused at the minimum rate required to keep the vein open, so that a negligible amount of fluid was infused (less than 100 ml).

Participants arrived in the sleep laboratory at noon for a daytime sleep study following a night of sleep deprivation of less than 4 h to facilitate the induction of sleep during the day. Participants refrained from consuming caffeinated beverages and alcohol at least 12 h prior to the experiments. Participants were instrumented for polysomnography. Before and after sleep, NC and UA-XSA were measured while lying in supine position.

2.2. Participants

Participants were recruited by advertisement. The inclusion criteria were as follows: nonobese men, with a body mass index less than 30 kg/m^2 and blood pressure less than 140/90 mmHg. The exclusion criteria were a history of sleep apnea, cardiovascular, kidney, neurological or respiratory diseases, use of prescribed medication, and use of over-the-counter medication that might affect fluid retention.

2.3. Polysomnography

Polysomnography (PSG) was performed during the day to accommodate scheduling of the nurse required to insert the IV line into the study participant. Sleep stages and arousals were scored according to standard techniques and criteria [17]. Nasal airflow was recorded by the BiNAPS® nasal airflow/pressure transducer system (Salter Labs, USA). Arterial oxyhemoglobin saturation (SaO_2) was captured by pulse oximetry [1]. Apneas were defined as more than 90% reduction in nasal airflow or thoraco-abdominal motion from baseline, lasting more than 10 s. Hypopneas were defined as more than 30% reduction in airflow lasting more than 10 s, associated with a minimum 3% desaturation or an arousal from sleep [17]. Severity of sleep apnea was assessed by apnea-hypopnea index (number of apneas and hypopneas per hour of sleep or AHI). Participants slept supine for the study period to eliminate the effect of different sleep postures.

2.4. Neck circumference and upper-airway cross-sectional area

Before and after sleep with participant supine, NC and UA-XSA were measured. NC was measured by a tape measure just above the cricothyroid cartilage [16]. A mark was drawn at the same level to ensure consistency of the repeated measurement after sleep. UA-XSA was assessed by acoustic pharyngometry [18].

2.5. Ethics statement

The Research Ethics Board of Toronto Rehabilitation Institute approved this protocol. All participants provided written consent prior to participation.

2.6. Signal processing

Signal processing included four main stages: (1) preprocessing the recorded nasal airflow, (2) extracting physiology-driven features, (3) using the extracted features to classify every breath into normal or flow limited breaths, and (4) validation of the classification results. These methods are outlined in Fig. 1.

2.6.1. Preprocessing

The nasal airflow was sampled at 85.33 Hz. The frequency of the recorded airflow ranged from 0.01 Hz to 3.2 Hz. The data were first preprocessed, which includes denoising and respiratory onset detection. UA collapsibility and the control mechanisms of UA dilator muscles are highly dependent on the sleep stage [19]. To account for this state-dependence and because all participants spent most of the time in non-rapid eye movement stage 2 (N2) sleep [20], only nasal airflow data captured during N2 sleep were included.

To denoise the signal, three different methods were compared and the most optimal method was selected. These methods include filtering with a Gaussian function, a low-pass Butterworth filter, and a wavelet denoising filter with symlet-4 function. The filter parameters were chosen in order to remove the noise and smooth

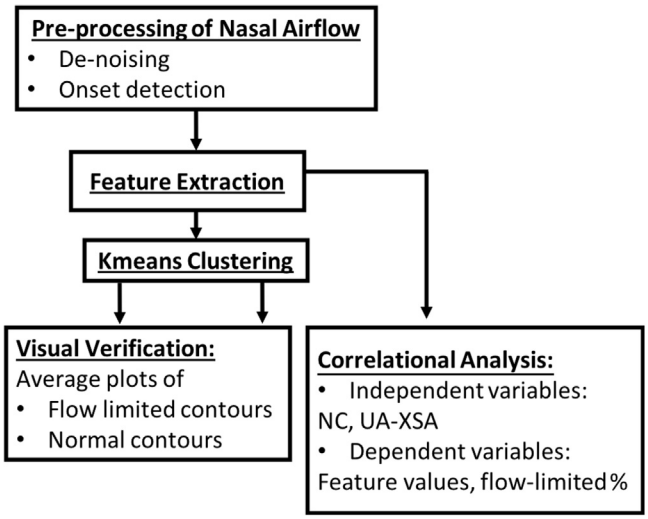

Fig. 1. Schematic illustration of the signal processing method. The nasal airflow was first preprocessed with denoising and onset detection algorithms. The nasal airflow of each inspiratory period was partitioned into inspiratory contours, based on which features were extracted. The feature results were used as the inputs for k-means clustering. Two clusters – flow limited and normal – were generated. The contours of those two clusters were averaged for visual verification. In addition, the correlations were calculated between the independent variables: neck circumference (NC) and upper-airway cross-sectional area (UA-XSA) and the dependent variables: feature values and percentage of breaths considered to be flow limited (flow-limited %).

the signal, while preserving the main features of the original signal such as its histogram. The performance of various filters was compared using simulated noisy airflow (for details, please refer to the Supplementary Materials).

An important step for feature extraction and classification is the accurate detection of inspiratory and expiratory onsets. Onset detection can be challenging because the baseline of the nasal airflow signal can shift due to head movement, technical difficulties with sensor design, and air leakage from the sensor. We developed an algorithm based on analyzing variations in the slope of nasal airflow to automatically account for the changes in nasal airflow baseline over time (for details, please refer to the Supplementary Materials). Furthermore, we implemented three methods based on the previous literature: median of the signal [21], prespecified constant baseline of the nasal airflow [22], and maximum rate of change [1].

The denoising and onset detection methods together influence onset detection results. Therefore, different denoising methods were combined with different onset detection algorithms to automatically locate onsets. The results were compared with the onsets identified manually on the unfiltered data and inspiratory onset errors were calculated. The combination of denoising and onset detection algorithm with the smallest error would be recommended for preprocessing (for details, please refer to the Supplementary Materials).

2.6.2. Feature extraction

Five features were extracted to describe the temporal patterns of the inspiratory airflow. The selection of features was inspired by the relevant literature as well as visual observation.

1. Deviation index [10] which describes how much the nasal airflow deviates from an ideal contour during normal inspiration. Deviation index is estimated as the difference between the area under an airflow contour ($A_{airflow}$) measured during inspiration and the area under a normal airflow contour which was simulated as a sinusoidal waveform ($A_{sinusoid}$) with similar peak amplitude and duration to the nasal airflow (Fig. 2a). Only the middle 50% of airflow contour was used for calculating deviation index as it was shown that the middle portion of the airflow contour is most indicative of flow limitation [1]:

$$Deviation\ Index = \frac{\left|A_{airflow} - A_{sinusoid}\right|}{A_{airflow}} \quad (1)$$

2. Peak amplitude variability, which represents variations in the amplitude of airflow. Presence of apneas, hypopneas, and the following hyperventilation periods increase variability of airflow amplitude in sleep-disordered breathing compared to normal breathing. Peak amplitude variability is calculated as the peak amplitude of nasal airflow (F_{peak}) normalized by the average (arithmetic mean) peak amplitude of the nasal airflow over all breaths (Avg_{peak}, Fig. 2b).

$$Peak\ Amplitude\ Variability = \frac{F_{peak}}{Avg_{peak}} \quad (2)$$

3. Scooping index [23] was shown to indicate transient increases in the UA collapsibility during inspiration. It is calculated as the difference between the first trough (F_{trough}) and peak of the nasal airflow (F_{peak}) divided by the peak of nasal airflow (Fig. 2c) [23–25].

$$Scooping\ Index = \frac{F_{peak} - F_{trough}}{F_{peak}} \quad (3)$$

4. Peak number in every inspiratory contour (Fig. 2d). Having more than one peak during inspiration indicates snoring which is associated with the UA narrowing.
5. Kurtosis of the inspiratory contour, equivalent to the "peakedness" of the signal (Fig. 2e). For example, Kurtosis of a normal airflow with a bell shape is three, while Kurtosis of a flattened airflow is less than three. Therefore, a flattened contour during flow limitation will yield a smaller kurtosis compared to a rounded contour associated with normal breathing:

$$Kurtosis = \frac{E(x-\mu)^4}{\sigma^4} \quad (4)$$

where μ is the mean and σ is standard deviation of the airflow contour.

2.6.3. Unsupervised clustering

In this study, we did not use esophageal manometry to detect flow limited breaths. Therefore, we implemented an unsupervised classification algorithm based on k-means clustering (k = 2) to classify every breath as either normal or flow limited. K-means clustering is an iterative process which starts with k initial random "means" (also known as cluster centroids). In every iteration, the algorithm updates the clusters by assigning the features of each inspiratory contour to the closest cluster centroid based on the Euclidean distance. Then, the cluster centroids were updated as the average of the classified features within each cluster. This process was repeated until the total sum of distance from centroids did not change.

The adequacy of the k-means classifier in separating the data into distinct groups was described using measures of separability. We report separability as statistical differences between the

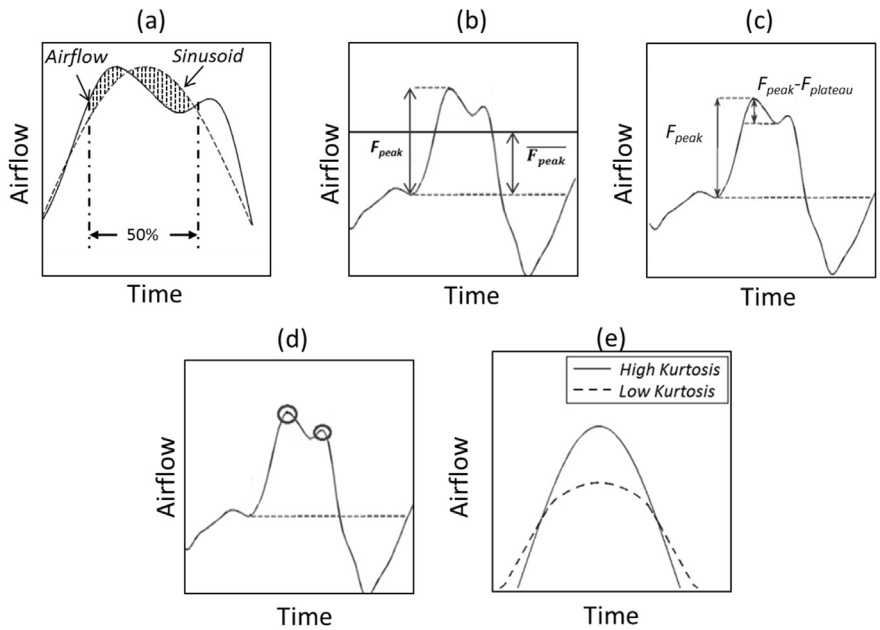

Fig. 2. Graphical representation of the following features: (a) Deviation Index, (b) Peak Amplitude Variability, (c) Scooping Index, (d) Peak Number, and (e) Kurtosis.

clusters for each feature and participant. Statistical differences were computed using the unpaired t-test. In addition, we utilized the Silhouette method to validate the consistency of clusters within the data across all features [26]. This method outputs a single value that is an aggregate measure of similarity between each data point and the cluster to which it is assigned, compared to the neighboring cluster. The silhouette ranges from −1 to 1, where a value closer to 1 indicates that the samples are well matched to their own clusters and poorly matched to neighboring clusters.

K-means clustering is sensitive to the absolute magnitude the data which can vary across features with incomparable units. To correct for this, input features were converted to z-scores, such that each feature had a mean of 0 and standard deviation of 1. K-means clustering is also sensitive to the initial selection of cluster centroids and may terminate at local minima. To overcome this issue, the clustering algorithm was repeated 100 times with different initial centroids. The histogram of centroids from 100 repetitions was generated and two centroids with maximum frequency of repetition were selected as the cluster centroids for normal and flow limited classes. Finally, based on these centroids, Euclidean distance of each inspiratory contour to the cluster centroid was used to classify the inspiratory contours into normal or flow limited classes.

To validate classification results, for every participant, the average and standard deviation of all inspiratory contours within normal or flow limited clusters were calculated. These average contours were visually compared with those from the previous literature. The percentage of flow limited breaths (flow-limitation %) was defined as the number of inspiratory contours clustered as flow limited divided by the total number of inspiratory contours.

2.7. Statistical analysis

We investigated the correlation between the extracted features and the UA anatomical variables including baseline NC, UA-XSA, and ΔNC, ΔUA-XSA after sleep. Similarly, we investigated the correlations between flow-limitation % and the baseline NC, UA-XSA, and ΔNC, ΔUA-XSA after sleep.

Normality of the data was first tested with the Anderson–Darling test. Pearson correlations were applied for normally distributed data and Spearman's rank correlations for non-normally distributed data. A correlation is considered significant with a two-tailed p-value <0.05. All data are reported as mean ± SD.

All the signal processing and statistical analyses were conducted with Matlab® R2014a.

3. Results

Sixteen nonobese men, aged 39.9 ± 14.0 years and with an AHI of 21.7 ± 25.2 events/hour completed the protocol with total sleep time of 136 ± 50 min. Because of technical difficulties, one and two out of the 16 participants did not have measurements of NC and UA-XSA, respectively. Participant demographics are shown in Table 1. On an average, 1080 ± 448 inspiratory airflow contours were investigated from each participant during N2 sleep.

Among all the combinations of preprocessing filters and onset detection algorithms, the onset detection algorithm based on our proposed method combined with Gaussian low-pass filter achieved the smallest errors compared to the manually determined onsets (details are presented in the supplementary information, Table S2).

The peak amplitude variability was strongly and positively correlated with ΔNC (Fig. 3a). There was also a strong negative correlation between the peak amplitude variability and baseline UA-XSA (Fig. 3b). The significant correlations were preserved even after removing the potential outlier whose peak amplitude

Table 1
Participant demographics.

Number of participants	16
Age, years	40 ± 14
Height, cm	175.0 ± 5.9
Weight, kg	83.2 ± 10.5
Body mass index, kg/m^2	27.4 ± 2.9
Neck circumference, cm	42.8 ± 2.5
Upper airway cross-sectional area, cm^2	2.6 ± 0.6
Heart rate, bpm	70 ± 9
Apnea-hypopnea index, events/hour sleep	21.7 ± 25.2

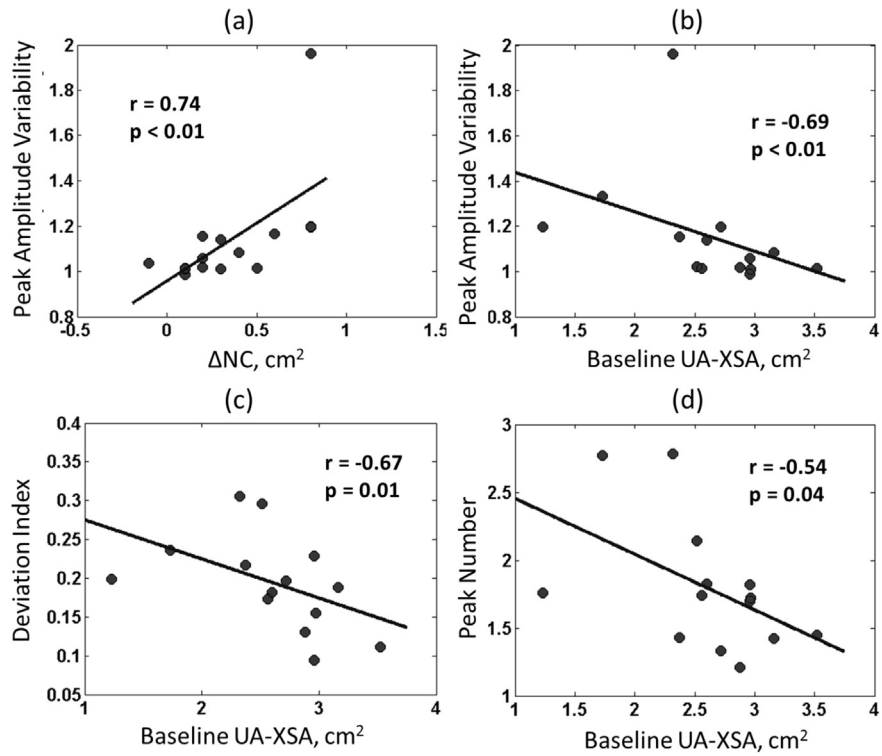

Fig. 3. (a) Peak amplitude variability is positively and strongly correlated with ΔNC (NC: neck circumference), and (b) negatively and strongly correlated with baseline UA-XSA (upper airway cross-sectional area); (c) deviation index is negatively and significantly correlated with baseline UA-XSA; and (d) peak number is negatively and significantly correlated with baseline UA-XSA.

variability was close to 2. Deviation index was significantly and negatively correlated with baseline UA-XSA (Fig. 3c). The peak number was significantly and negatively correlated with baseline UA-XSA (Fig. 3d). Lastly, scooping index was negatively correlated with ΔNC (Table 2). There was no correlation between kurtosis and any of the independent variables (Table 2).

Fig. 4 shows the mean and standard deviation contours of apparent flow limited and normal clusters for every individual. The solid curves indicate the mean contour and the dashed curves indicate mean ± SD curves. It can be seen that for most of the participants, the apparent flow limited contours contain obvious flattening and apparent normal flow contours contain rounded bell shape, with the exception of participant 10 whose flow limited contour contains rounded bell shape with only slight steady slope.

Table 3 shows the results of the t-test describing separability of the clusters for each feature and participant. In addition, the silhouette coefficient describes overall separability, which accounts for all features in a single metric for each participant. Nearly all the individual features were significantly different between the clusters across participants. Only peak amplitude variability was not significantly different between the clusters for participants 1, 3, 13, and 16. Furthermore, deviation index, scooping index, peak number, and kurtosis were all higher in the flow limited cluster, compared to the normal cluster across all participants. Peak amplitude variability was generally lower in the flow limited cluster across most participants. Overall separability measured by the silhouette analysis was greater than 0 for all participants and greater than or equal to 0.4 in 13 of 16 participants.

Fig. 5 shows the correlations between flow-limitation % and baseline UA-XSA. Participants with narrower UA before sleep had a significantly greater percentage of flow limited breaths. There was no significant correlation between flow-limitation % and other measured variables.

4. Discussion

This study has led to several important and novel findings with implications for sleep physiology. First, we have shown that temporal features of the nasal airflow contours, such as peak amplitude variability, deviation index, and peak number were strongly correlated with the neck and UA anatomical measurements such as NC and UA-XSA. Second, clustering based on these features resulted in two clusters corresponding to normal, round contours, and flow limited contours containing flattened regions. Third, we found that the percentage of breaths inferred as flow limited was strongly correlated with UA-XSA before sleep, an index of UA narrowing [27]. To our knowledge, this is the first study that investigated the relationship between features of the airflow contours and UA

Table 2
Correlations, r (p), between proposed features and airway anatomic variables. NC: neck circumference; UA-XSA: upper airway cross-sectional area.

	Deviation index	Peak amplitude variability	Peak number	Scooping index	Kurtosis	IFL (%)
NC	0.06 (0.84)	0.17 (0.57)	−0.1 (0.72)	−0.07 (0.81)	0.11 (0.69)	0.39 (0.15)
ΔNC	0.37 (0.17)	0.74 (<0.01)	0.2 (0.36)	−0.57 (0.03)	−0.11 (0.67)	0.43 (0.11)
UA-XSA	−0.67 (0.01)	−0.69 (<0.01)	−0.54 (0.04)	0.42 (0.13)	−0.18 (0.55)	−0.53 (0.05)
ΔUA-XSA	0.22 (0.45)	0.08 (0.78)	0.37 (0.27)	0.23 (0.44)	0.17 (0.56)	0.31 (0.28)

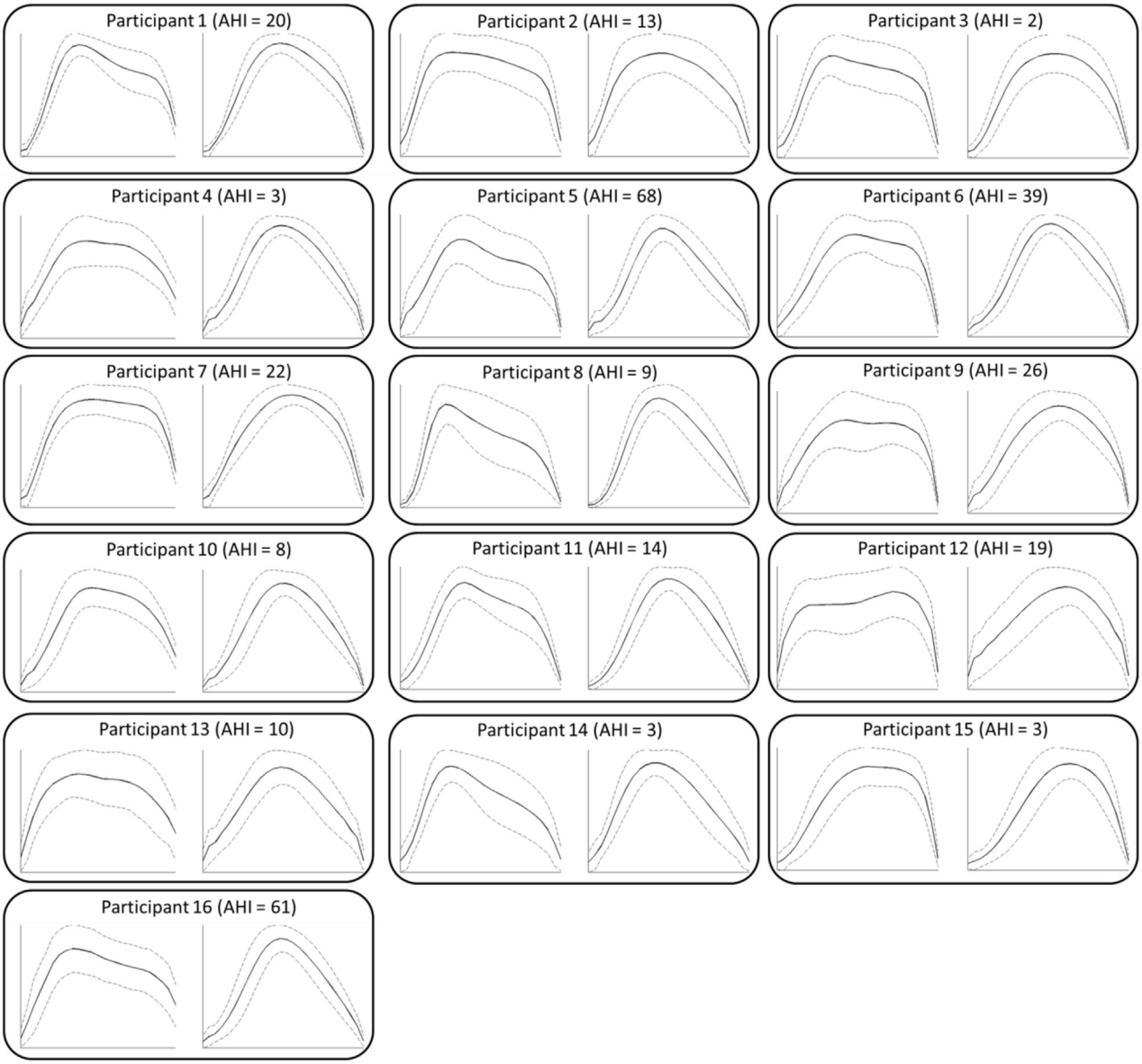

Fig. 4. The average contour plots ± standard deviations for the 16 participants. For each participant, the contours on the left side are considered flow limited and the contours on the right side are considered normal.

anatomy. These results demonstrate that features of the airflow contour are associated with UA narrowing and demonstrate potential for detecting flow limitation.

Manual detection of flow limited breaths largely relies on the visual identification of flattening or scooping in inspiratory airflow contours [28,29]. However, those visual features have not been validated with respect to the anatomical properties of the UA. In the present study, we proposed five temporal features of nasal airflow and showed that three features including peak amplitude variability, deviation index, and peak number were strongly correlated with UA narrowing, indicating their potential physiological relevance. Specifically, the peak amplitude variability represents the extent of variation of flow amplitude. Highly variable flow amplitude commonly appears during the hyperventilatory period following apneas and hypopneas. In the present study, a greater flow variability was associated with a narrower UA-XSA and more overnight change in NC. Additionally, the deviation index and peak number were both negatively correlated with baseline UA-XSA indicating that a higher deviation index and more peaks in the airflow contour were associated with a narrower UA. This is consistent with flow limitation since the deviation index describes the extent to which the airflow contour deviates from ideal airflow during normal inspiration, while the presence of multiple peaks in the airflow contour could be attributed to snoring, soft tissue vibration during inspiration, or UA reopening after a partial closure [11,21]. Overall, these features together can be a powerful analytical metric for investigation of the UA pathophysiology.

The results from k-means clustering further confirm some of the results of the correlation analysis. For example, deviation index and peak number were both greater in the apparent flow limitation cluster, which is consistent with flow limited breathing and the relationship of these features with the anatomical properties of the UA. Similarly, while scooping index did not correlate with properties of the UA, it was greater in the apparent flow limited cluster, which is also consistent with the airflow contour of flow limited breaths. Unexpectedly, kurtosis was higher and peak amplitude

Table 3
Mean and standard deviation values of each feature to describe differences between clusters representing flow limited and normal breaths.

Participant	Deviation index		Peak amplitude variability		Scooping index		Peak number		Kurtosis		Silhouette coefficient
	Flow limited	Normal	Flow limited	Normal	Flow limited	Normal	Flow limited	Normal	Flow limited	Normal	
1	0.30 ± 0.22	0.09 ± 0.06*	1.12 ± 0.95	1.06 ± 0.37	2.87 ± 2.15	1.11 ± 0.34*	0.28 ± 0.28	0.00 ± 0.02*	2.23 ± 0.56	1.71 ± 0.17*	0.80
2	0.41 ± 0.47	0.16 ± 0.10*	0.90 ± 0.55	1.22 ± 0.68*	2.72 ± 1.28	1.11 ± 0.39*	0.27 ± 0.29	0.00 ± 0.02*	2.24 ± 0.52	1.71 ± 0.20*	0.64
3	0.15 ± 0.11	0.09 ± 0.07*	1.04 ± 0.39	1.00 ± 0.35	2.06 ± 0.27	1.10 ± 0.32*	0.35 ± 0.21	0.00 ± 0.02*	2.44 ± 0.45	1.98 ± 0.29*	0.62
4	0.28 ± 0.51	0.14 ± 0.09*	1.01 ± 0.64	1.90 ± 2.01*	3.46 ± 1.40	1.45 ± 0.73*	0.09 ± 0.18	0.01 ± 0.03*	2.90 ± 0.77	2.02 ± 0.36*	0.40
5	0.30 ± 0.42	0.11 ± 0.07*	0.97 ± 0.75	1.22 ± 0.57*	2.87 ± 2.52	1.46 ± 0.61*	0.19 ± 0.24	0.01 ± 0.04*	2.74 ± 1.41	1.97 ± 0.29*	0.20
6	0.26 ± 0.50	0.11 ± 0.08*	0.82 ± 0.71	1.07 ± 0.42*	2.32 ± 0.57	1.18 ± 0.45*	0.27 ± 0.26	0.01 ± 0.03*	2.43 ± 0.66	1.72 ± 0.23*	0.65
7	0.34 ± 0.39	0.10 ± 0.07*	0.84 ± 0.36	1.09 ± 0.33*	2.92 ± 1.28	1.24 ± 0.50*	0.17 ± 0.23	0.01 ± 0.03*	2.39 ± 0.54	1.89 ± 0.28*	0.56
8	0.28 ± 0.25	0.11 ± 0.09*	0.84 ± 0.33	1.03 ± 0.22*	2.28 ± 0.62	1.10 ± 0.31*	0.31 ± 0.26	0.00 ± 0.03*	2.28 ± 0.69	1.68 ± 0.21*	0.81
9	0.20 ± 0.16	0.12 ± 0.07*	0.90 ± 0.28	1.04 ± 0.21*	2.45 ± 0.60	1.37 ± 0.62*	0.27 ± 0.26	0.01 ± 0.04*	2.17 ± 0.36	1.69 ± 0.21*	0.48
10	0.41 ± 0.32	0.17 ± 0.14*	1.09 ± 1.25	2.70 ± 3.77*	4.07 ± 1.96	1.51 ± 0.68*	0.07 ± 0.18	0.01 ± 0.04*	2.72 ± 0.91	1.80 ± 0.28*	0.25
11	0.33 ± 0.25	0.15 ± 0.10*	0.98 ± 0.58	1.15 ± 0.62*	3.09 ± 1.31	1.27 ± 0.56*	0.14 ± 0.23	0.00 ± 0.03*	2.46 ± 0.67	1.76 ± 0.26*	0.50
12	0.21 ± 0.28	0.09 ± 0.08*	0.91 ± 0.52	1.29 ± 0.95*	2.25 ± 0.70	1.13 ± 0.35*	0.14 ± 0.17	0.00 ± 0.02*	2.88 ± 0.50	2.14 ± 0.39*	0.47
13	0.25 ± 0.16	0.12 ± 0.07*	1.05 ± 0.72	1.18 ± 0.83	2.48 ± 0.76	1.38 ± 0.67*	0.32 ± 0.30	0.01 ± 0.04*	2.18 ± 0.47	1.72 ± 0.22*	0.36
14	0.38 ± 0.34	0.17 ± 0.12*	0.81 ± 0.60	1.25 ± 0.92*	2.35 ± 0.72	1.20 ± 0.44*	0.16 ± 0.22	0.01 ± 0.03*	2.37 ± 0.56	1.67 ± 0.22*	0.48
15	0.34 ± 0.35	0.14 ± 0.09*	0.74 ± 0.54	1.33 ± 0.80*	3.63 ± 1.86	1.11 ± 0.41*	0.18 ± 0.26	0.00 ± 0.02*	2.65 ± 0.91	1.64 ± 0.18*	0.64
16	0.37 ± 0.29	0.12 ± 0.10*	1.08 ± 0.64	1.08 ± 0.39	2.44 ± 0.66	1.11 ± 0.35*	0.26 ± 0.29	0.00 ± 0.02*	2.40 ± 0.46	1.74 ± 0.22*	0.69

*P < 0.0001.

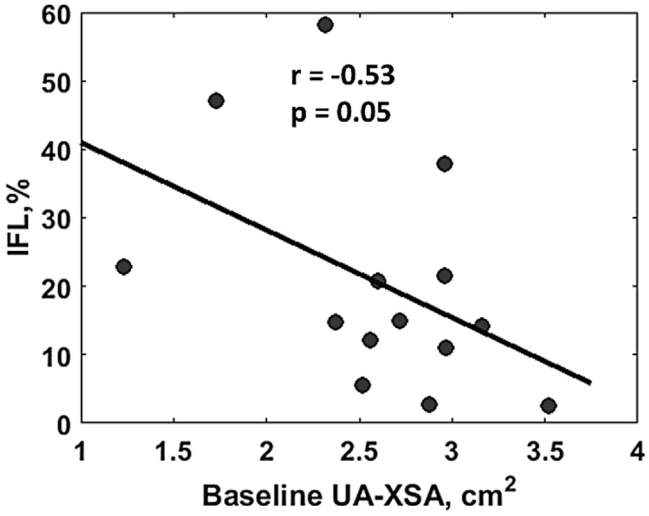

Fig. 5. Percentage of inspiratory flow limited breaths (flow-limitation %) was negatively and significantly correlated with baseline UA-XSA (UA-XSA: upper airway cross-sectional area).

variability was lower in the apparent flow limited cluster, compared to the normal cluster. We anticipated that kurtosis would be lower in the flow limited cluster given the more flattened shape of the flow limited airflow contour. Furthermore, greater variability in the peak amplitude was anticipated in the flow limited cluster, as this commonly appears in hyperventilatory period following apneas and hypopneas, as described previously. Future studies should therefore be cautious to include these features in a model to automatically detect flow limited breathing.

The k-means clustering algorithm is limited for the current application in that it divides breaths into either the flow limited or normal breaths, despite the presence or absence of flow limited breathing in a participant. It is impossible to know whether clusters included normal breaths in the flow limited cluster, or vice versa, without a ground truth measure of flow limitation. Given this limitation, we computed cluster separability, such that poor separability or overlapping clusters would indicate that k-means clustering likely forced a single type of breathing into two clusters. As shown in Table 3, the mean values of the features are statistically different between flow limited and normal breaths for nearly every participant. Moreover, the silhouette values are all greater than 0, and in fact greater than 0.4 for 13/6 participants indicating adequate separation. In addition, the mean values of the features in the flow limited cluster, compared to the normal cluster, are generally consistent with the characteristics of flow limited breathing, as described in the previous paragraph. Therefore, it is clear that the flow limited cluster is distinct from the normal cluster and that the breaths therein demonstrate characteristics consistent with flow limited breathing.

Statistical classifiers based on the airflow contour were developed in previous studies to automatically detect flow limited breathing with high accuracy. Yet, most of those classifiers were constructed from or validated by the invasive measurement of pharyngeal pressure or esophageal pressure, which can be cumbersome to perform routinely [1,22,24]. Previous studies have proposed supervised [10] and unsupervised [11,21] algorithms to detect flow limitation. However, the relationship between the abnormal flow contours and UA narrowing was not investigated.

In our study, we discovered the features of airflow that are correlated with UA narrowing. We also demonstrated the presumed relationship between the degree of UA narrowing and the frequency of flow limitation. We showed that the narrower the UA

before sleep, the more frequently flow limited breathing occurred. This is consistent with the previous study indicating that prolonged flow limitation of more than 30% of total sleep time is associated with palatal anatomical abnormalities such as a thick palate, lateral pharyngeal wall, or uvula in patients with mild sleep-disordered breathing [4]. Our finding justifies the possibility of predicting UA narrowing noninvasively with convenient airflow monitoring [16,30,31].

The potential clinical application of this research is significant. The standard metrics for assessing the severity of OSA include apneas, hypopneas, arousals, and oxygen desaturation. However, these metrics are found to be weakly correlated or not correlated with the clinical symptoms of sleep-disordered breathing in certain populations such as pregnant women and children [32]. For instance, frequent presence of flow limitation and arousals is associated with gestational hypertension and diabetes in pregnant women [33,34]. Furthermore, in the pediatric population, even simple snoring with persistent flow limitation, but without elevated AHI, has been related to impaired cognitive function and reduced social-behavioral performance [35–37]. Therefore, flow limitation has been increasingly recognized as a breathing pattern for the assessment of sleep-disordered breathing which cannot be determined based on traditional definition of apneas and hypopneas [32]. By leveraging the noninvasive nasal airflow recording and an automated classification program, we can develop algorithms to evaluate milder, but usually prolonged degrees of inspiratory flow limitation in susceptible populations such as pregnant women and children. The proposed algorithm will have the potential to complement the existing diagnostic criteria for sleep related breathing disorders and help develop more appropriate and personalized treatments to optimize clinical outcomes.

The present study is limited in that flow limitation during respiratory event-related arousals (RERAs) were not isolated and analyzed. Flow limitation may have more relevant clinical outcomes in association with RERA rather than hypopnea [32]. However, the focus of this research is to identify features that differentiate normal breaths from those with inspiratory flow limitation. Investigating the potential differences between contours of flow limited breaths during RERA versus hypopnea is an important question which can be studied in future. In addition, the features investigated were validated on data of nonobese men, and the results may not be applicable to other populations with inspiratory flow limitation, such as children, obese individuals, and pregnant women. Future studies could validate the proposed features in a wider range of individuals at risk of inspiratory flow limitation.

This study is subject to additional limitations: (1) When shallow breathing or mouth breathing occur, signal amplitude is low and respiratory onsets become more ambiguous. As a result, the accuracy of feature extraction is compromised. (2) Currently the onset detection was validated against manual identification of onsets, which may not accurately represent the true onsets. (3) Another challenge of this study is the lack of pharyngeal pressure measurement, which is considered as the standard assessment of flow limitation. (4) Finally, the study was performed during the daytime, which may differ from overnight sleep.

In conclusion, we investigated a set of airflow features capable of objective detection of flow limitation from the nasal airflow signal. With this method, we demonstrated that the frequency of flow limitation is strongly correlated with UA narrowing. Because the features are extracted from nasal airflow, which is commonly recorded in full in-laboratory polysomnography and most portable systems for sleep monitoring, they can be easily implemented in various sleep studies in the laboratory and at home. The investigated features can be used to develop a classification model for accurate detection of flow limitation and applied in larger clinical trials to assess the association between flow limitation and health outcomes, such as pregnancy complications and birth outcomes in pregnant women or cognitive function in children who do not have sleep apnea, but may have flow limitation (See Ref. [38]).

Acknowledgement

The research leading to these results has received partial funding from Sleep and Biological Rhythms Toronto, a CIHR funded research and training program.

Y.X.Z. was supported by the Sleep and Biological Rhythms Toronto, a CIHR funded research and training program, and the Toronto Rehabilitation Institute scholarship.

T.D.B. was supported by the Clifford Nordal Chair in Sleep Apnea and Rehabilitation Research and the Godfrey S. Pettit Chair in Respiratory Medicine.

Conflict of interest

The ICMJE Uniform Disclosure Form for Potential Conflicts of Interest associated with this article can be viewed by clicking on the following link: https://doi.org/10.1016/j.sleep.2018.04.006.

Appendix A. Supplementary data

Supplementary data related to this article can be found at https://doi.org/10.1016/j.sleep.2018.04.006.

References

[1] Clark SA, Wilson CR, Satoh M, et al. Assessment of inspiratory flow limitation invasively and noninvasively during sleep. Am J Respir Crit Care Med 1998;158(3):713–22.
[2] Rimpilä V, Saaresranta T, Huhtala H, et al. Transcutaneous CO(2) plateau as set-point for respiratory drive during upper airway flow-limitation. Respir Physiol Neurobiol 2014;191:44–51.
[3] Tsara V, Amfilochiou A, Papagrigorakis M, et al. Definition and classification of sleep related breathing disorders in adults: different types and indications for sleep studies (Part 1). Hippokratia 2009;13(3):187.
[4] de Godoy LB, Palombini LO, Haddad FLM, et al. New insights on the pathophysiology of inspiratory flow limitation during sleep. Lung 2015;193(3):387–92.
[5] Pamidi S, Redline S, Rapoport D, et al. An Official American thoracic Society Workshop report: noninvasive identification of inspiratory flow limitation in sleep studies. Ann Am Thorac Soc 2017;14(7):1076–85.
[6] Flemons W, Buysse D, Redline S, et al. Sleep-related breathing disorders in adults: recommendations for syndrome definition and measurement techniques in clinical research. Sleep 1999;22(5):667–89.
[7] Guilleminault C, Stoohs R, Clerk A, et al. A cause of excessive daytime sleepiness: the upper airway resistance syndrome. Chest 1993;104(3):781–7.
[8] Hosselet JJ, Norman RG, Ayappa I, et al. Detection of flow limitation with a nasal cannula/pressure transducer system. Am J Respir Crit Care Med 1998;157(5 Pt 1):1461–7.
[9] Montserrat JM, Farré R, Ballester E, et al. Evaluation of nasal prongs for estimating nasal flow. Am J Respir Crit Care Med 1997;155(1):211–5.
[10] Norman RG, Rapoport DM, Ayappa I. Detection of flow limitation in obstructive sleep apnea with an artificial neural network. Physiol Meas 2007;28(9):1089.
[11] Aittokallio T, Saaresranta T, Polo-Kantola P, et al. Analysis of inspiratory flow shapes in patients with partial upper-airway obstruction during sleep. CHEST J 2001;119(1):37–44.
[12] Friedman O, Bradley TD, Chan CT, et al. Relationship between overnight rostral fluid shift and obstructive sleep apnea in drug-resistant hypertension. Hypertension 2010;56(6):1077–82.
[13] Kasai T, Motwani SS, Yumino D, et al. Differing relationship of nocturnal fluid shifts to sleep apnea in men and women with heart failure. Circulation – Heart Fail 2012;5(4):467–74.
[14] Redolfi S, Yumino D, Ruttanaumpawan P, et al. Relationship between overnight rostral fluid shift and obstructive sleep apnea in nonobese men. Am J Respir Crit Care Med 2009;179(3):241–6.
[15] Shepard Jr JW, Pevernagie DA, Stanson AW, et al. Effects of changes in central venous pressure on upper airway size in patients with obstructive sleep apnea. Am J Respir Crit Care Med 1996;153(1):250–4.

[16] Yadollahi A, Gabriel JM, White LH, et al. A randomized, double crossover study to investigate the influence of saline infusion on sleep apnea severity in men. Sleep 2014;37(10):1699–705.
[17] Berry RB, Budhiraja R, Gottlieb DJ, et al. Rules for scoring respiratory events in sleep: update of the 2007 AASM Manual for the Scoring of Sleep and associated events. Deliberations of the sleep apnea definitions task force of the American academy of sleep medicine. J Clin Sleep Med 2012;8:597–619.
[18] Fredberg JJ, Wohl M, Glass GM, et al. Airway area by acoustic reflections measured at the mouth. J Appl Physiol 1980;48(5):749–58.
[19] Leung RST, Comondore VR, Ryan CM, et al. Mechanisms of sleep-disordered breathing: causes and consequences. Pflügers Archiv – Eur J Physiol 2011;463(1):213–30.
[20] Yadollahi A, Vena D, Lyons OD, et al. Relationship of fluid accumulation in the neck to sleep structure in men during daytime sleep. J Clin Sleep Med 2016:1365–71.
[21] Aittokallio T, Malminen JS, Pahikkala T, et al. Inspiratory flow shape clustering: an automated method to monitor upper airway performance during sleep. Comput Methods Programs Biomed 2007;85(1):8–18.
[22] Morgenstern C, Jane R, Schwaibold M, et al. Automatic classification of inspiratory flow limitation assessed non-invasively during sleep. Conf Proc IEEE Eng Med Biol Soc 2008;2008:1132–5.
[23] Owens RL, Edwards BA, Sands SA, et al. The classical Starling resistor model often does not predict inspiratory airflow patterns in the human upper airway. J Appl Physiol 2014;116(8):1105–12.
[24] Mansour KF, Rowley JA, Badr MS. Noninvasive determination of upper airway resistance and flow limitation. J Appl Physiol (1985) 2004;97(5):1840–8.
[25] Morgenstern C, Jane R, Schwaibold M, et al. Characterization of inspiratory flow limitation during sleep with an exponential model. In: 2008 30th Annual International Conference of the IEEE Engineering in Medicine and Biology Society. IEEE; 2008.
[26] Rousseeuw PJ. Silhouettes: a graphical aid to the interpretation and validation of cluster analysis. J Comput Appl Math 1987;20:53–65.
[27] Gavrilovic B, Bradley TD, Vena D, et al. Factors predisposing to worsening of sleep apnea in response to fluid overload in men. Sleep Med 2016;23:65–72.
[28] Ayappa I, Norman R, Krieger A, et al. Non-Invasive detection of respiratory effort-related arousals (REras) by a nasal cannula/pressure transducer system. Sleep 2000;23(6):763.
[29] Condos R, Norman RG, Krishnasamy I, et al. Flow limitation as a noninvasive assessment of residual upper-airway resistance during continuous positive airway pressure therapy of obstructive sleep apnea. Am J Respir Crit Care Med 1994;150(2):475–80.
[30] Shiota S, Ryan CM, Chiu K-L, et al. Alterations in upper airway cross-sectional area in response to lower body positive pressure in healthy subjects. Thorax 2007;62(10):868–72.
[31] Yadollahi A, Singh B, Bradley TD. Investigating the dynamics of supine fluid redistribution within multiple body segments between men and women. Ann Biomed Eng 2015:1–12.
[32] Arora N, Meskill G, Guilleminault C. The role of flow limitation as an important diagnostic tool and clinical finding in mild sleep-disordered breathing. Sleep Sci 2015;8(3):134–42.
[33] Connolly G, Razak A, Hayanga A, et al. Inspiratory flow limitation during sleep in pre-eclampsia: comparison with normal pregnant and nonpregnant women. Eur Respir J 2001;18(4):672–6.
[34] Pamidi S, Pinto LM, Marc I, et al. Maternal sleep-disordered breathing and adverse pregnancy outcomes: a systematic review and metaanalysis. Am J Obstet Gynecol 2014;210(1):52. e1-52. e14.
[35] O'Brien LM, Holbrook CR, Mervis CB, et al. Sleep pressure correlates of cognitive and behavioral morbidity in snoring children. Sleep 2004;27(2):279–82.
[36] Kennedy J, Blunden S, Hirte C, et al. Reduced neurocognition in children who snore. Pediatr Pulmonol 2004;37(4):330–7.
[37] O'Brien LM, Holbrook CR, Mervis CB, et al. Sleep and neurobehavioral characteristics of 5-to 7-year-old children with parentally reported symptoms of attention-deficit/hyperactivity disorder. Pediatrics 2003;111(3):554–63.
[38] Chourasia V, Mittra A. Selection of mother wavelet and denoising algorithm for analysis of foetal phonocardiographic signals. J Med Eng Technol 2009;33(6):442–8.